

# An Adaptive Dimensionality Reduction Approach for Hyperspectral Imagery Semantic Interpretation

Akrem Sellami, Imed Riadh Farah, Basel Solaiman

**Abstract**—With the development of HyperSpectral Imagery (HSI) technology, the spectral resolution of HSI became denser, which resulted in large number of spectral bands, high correlation between neighboring, and high data redundancy. However, the semantic interpretation is a challenging task for HSI analysis due to the high dimensionality and the high correlation of the different spectral bands. In fact, this work presents a dimensionality reduction approach that allows to overcome the different issues improving the semantic interpretation of HSI. Therefore, in order to preserve the spatial information, the Tensor Locality Preserving Projection (TLPP) has been applied to transform the original HSI. In the second step, knowledge has been extracted based on the adjacency graph to describe the different pixels. Based on the transformation matrix using TLPP, a weighted matrix has been constructed to rank the different spectral bands based on their contribution score. Thus, the relevant bands have been adaptively selected based on the weighted matrix. The performance of the presented approach has been validated by implementing several experiments, and the obtained results demonstrate the efficiency of this approach compared to various existing dimensionality reduction techniques. Also, according to the experimental results, we can conclude that this approach can adaptively select the relevant spectral improving the semantic interpretation of HSI.

**Keywords**—Band selection, dimensionality reduction, feature extraction, hyperspectral imagery, semantic interpretation.

## I. INTRODUCTION

**N**OWADAYS, with the development of hyperspectral remote sensing imaging technology, we can capture HSI with hundreds of contiguous bands across the electromagnetic spectrum. The HSI, referred to as "data cube", is a kind of 3-D datum with two spatial dimensions and one spectral dimension. A large number of spectral bands can better identify and distinguish different materials and map the constituents of the Earth's surface through hyperspectral analysis. Every pixel in a hyperspectral image can be represented as a high-dimensional vector across spectral dimensions. This detailed spectral information makes it possible to discriminate materials of interest more accurately. Although the high dimension brings many merits for using HSI, the huge storage requirement and computation burden make it hardly to be used in many practical situations.

A. Sellami and I. R. Farah are with RIADI Laboratory, National School of Computer Science, Manouba, Tunisia 2010 and the ITI Department, Telecom Bretagne, Brest-Iroise 29238 France (e-mail: akrem.sellami@telecom-bretagne.eu, imed.farah@telecom-bretagne.eu).

B. Solaiman is with ITI Department, Telecom Bretagne, Brest-Iroise 29238 France (e-mail: basel.solaiman@telecom-bretagne.eu).

Also, the high number of spectral bands and the low number of training samples pose the problem of the curse of dimensionality [1]. Different substances in a hyperspectral image exhibit distinctive spectral signatures. The use of HSI is becoming more and more widespread, such as target detection, changes detection, and object classification [2], [3]. Therefore, the semantic interpretation is a challenge task for HSI analysis, when it consists to extract the semantics information of data. In fact, the general goal is to assign a means of the different entity and to understand the content of the HSI, i.e. the description of the HSI content (objects, pixels,...) with symbols [4], [5] and to detect the different spatial relationships between the pixels and objects of HSI, i.e. the detection of distance, direction and topological relationships. However, the main issue of the HSI semantic interpretation is what information can be exploited and how can the relevant information be selected to improve the HSI semantic interpretation. Thus, the dimensionality reduction is an essential task to reduce the high dimensionality and to select the relevant spectral bands in order to improve the semantic interpretation of HSI. Aiming to resolve these issues, we present, in this paper, an adaptive dimensionality reduction approach for HSI semantic interpretation that allows to reduce the high dimensionality of HSI and to describe the contents of objects and the pixels neighbors using both techniques of dimensionality reduction.

This paper is organized as follows: In Section II, we present the existing works in the literature related to the dimensionality reduction of HSI. Section III presents the presented approach showing the different phases. In fact, we introduce the multi-linear algebra model based on the Tensor Locality Preserving Projection (TLPP) method as well as the extracted adjacency graph from TLPP method. Then, we go into details about adaptive band selection based on the weighted matrix. In Section IV, we show experimental results of bands selection using our approach with a comparative study. We conclude and suggest some perspectives in the last section.

## II. RELATED WORK

Dimensionality reduction is commonly applied as a preprocessing step for HSI processing in order to reduce the number of the spectral bands and ensure a well-conditioned representation of the class-conditional statistics. The

high number of spectral bands of HSI leads to a remarkable increase in computational time and storage costs also may degrade classification accuracy [6]. Therefore, dimensionality reduction is a fundamental problem in HSI processing. It seeks to decrease computational complexity of input data while some desired intrinsic information of the data is preserved. The dimensionality reduction problem [7] can be defined as follows: Let us consider a HSI represented by  $N \times D$  matrix  $R$  consisting of  $N$  pixels  $i \in \{1, 2, \dots, N\}$  with the number of spectral bands  $D$ , and  $p$  its the low dimensionality (where  $p < D$ , and often  $p \ll D$ ). Intrinsic dimensionality means that the pixels in the reduced image  $Y$  are lying on or near a manifold with dimensionality  $p$  that is embedded in the  $D$ -dimensional space. Indeed, the dimensionality reduction methods reduce the HSI  $R$  while retaining as much as possible the relevant information. In fact the dimensionality reduction consists to extract (projection) or to select (selection) the  $p$  components or bands, with  $p \ll D$ , such that:

$$Y = f(R) \quad (1)$$

where  $Y$  is the reduced matrix,  $f$  is a reduction function and  $R$  is the spectral observation vector of HSI. Therefore, the dimensionality reduction is an important phase where the aim is to discard the redundant and the high number of spectral bands and make it less time consuming for HSI processing. The two main approaches for dimensionality reduction are band selection (primitive selection) and features extraction (band projection). The band selection method reduces the dimensionality by selecting a subset with the most of characteristics of original HSI [8]. In HSI, every spectral band corresponds to a 2-dimensional image, which can be considered as a feature. Depending on the availability of labeled samples, band selection techniques can be categorized as supervised and unsupervised. Supervised band selection methods use label information of patterns to perform selection of bands as the Mutual Information method (MI) [9], [10] selects the most discriminative bands by measuring the correlation with the class labels. Unsupervised band selection is used for dimensionality reduction [11], [12], when no labeled pattern is available. In practice, the collection of class labels in HSI needs the field exploration and verification by experts, which is expensive and difficult due to excessive labor cost. Thus, unsupervised methods are more practical for HSI processing. State-of-the-art methods for band selection of HSI in unsupervised manner are basically of two types: Ranking-based methods [13], [12] and clustering-based methods [14], [15]. Determining the most distinctive and informative bands depending on some statistical criteria (e.g., Kullback-Leibler divergence, skewness, kurtosis) is the basic idea behind ranking-based band selection methods. Then, top bands are selected by a given dimensionality or threshold. Some ranking-based methods for HSI present in

the literature are information divergence (ID)-based method [13], maximum variance-based principal component analysis (MVPCA) [12], and similarity-based band selection method [16]. Chang and Wang [13] proposed a constrained band selection (CBS) method. In CBS, when the band has large information divergence with other bands, it is higher priority. In [12], a weighted principal component (WPC) is devised as the criterion, and an adaptive thresholding algorithm based on moving control chart is used to determine the number of selected bands. Clustering-based methods [15], [9] perform clustering over bands to group them according to their redundancy, and select one representative band from each cluster of bands. There exists a few clustering-based band selection techniques for HSI in the literature like Wards linkage strategy using divergence linkage strategy using divergence (WaLuDi) or using mutual information (WaLuMI) [17], and band selection using affinity propagation (AP) [18]. The feature extraction method is based on data transformation [6], [19]. It reduces the dimensionality by transforming the original spectral bands from HSI using linear or non linear combinations into a new low-dimensional space through projection. In fact, in the linear projection the dimensionality reduction can be expressed as:

$$Y = T \times R \quad (2)$$

where  $T$  is the transformation matrix. Most traditional methods belong to the feature extraction category, such as Fisher's Linear Discriminant Analysis (FLDA) [20], Principal Component Analysis (PCA) [21], Locality Preserving Projections (LPP) [6], and Isometric Feature Mapping (ISOMAP) [22]. The main advantage of projection methods is their high discrimination power. Also, the first few features may contain most of the information whereas the remaining ones contain noisy information. However, these techniques change the physical means of HSI due to the transformation phase of the original spectral bands. For this reason, many works have been proposed in this literature to overcome these issues; Yan et al. [23] developed a novel approach based on general graph embedding framework for dimensionality reduction. This approach allows to represent each vertex of graph as a low-dimensional vector that embodies some geometric characteristics of the HSI. Ji et al. [24] proposed a method for HSI classification using the spatial and spectral information, in which the relationship between the different pixels is represented in a hypergraph model. Yuan *et al.* [25] presented a spatial hypergraph embedding model for dimensionality reduction. This model has been applied for HSI classification. Nevertheless, the main limitation of linear projection methods is that they do not preserve the non linearity of data, whereas for non-linear projection methods, they suffer from computational time complexity. So, the major deficiency of projection methods is that they are based

on matrix algebra and they represent the HSI as vectors, which may destroy the spatial information of neighboring pixels. They only rely on spectral properties, neglecting the spatial rearrangement. In this context, a tensor model has been proposed to jointly analyze spatial and spectral structures of original HSI [26]. Also, in order to preserve the spatial and spectral information, Sellami et al. [27] proposed a new approach called features extraction based on Tensor modelling and Locality Preserving Projections (TLPP) for HSI classification. In order to improve the semantic interpretation of HSI, we present in this paper an adaptive dimensionality reduction approach using TLPP method and band selection based on weight matrix to select the informative bands describing the contents of objects and the pixels neighbors.

### III. PROPOSED APPROACH

In this section, we present the approach and give more details for each phase. In fact, Fig. 1 shows the flowchart of the approach. Indeed, it is divided into three phases; in order to preserve the spatial information, the first phase consists to project the original HSI into a subspace using the Tensor Locality Preserving Projection (TLPP). Based on the adjacency graph used in projection with TLPP, a knowledge has been extracted for pixel neighbors description. Indeed, the spectral library has been used in this step to classify the different pixels. Then, the geodesic distance matrix has been applied to construct a weighted matrix between pixels. In fact, using this weighted matrix, the original spectral bands have been ranked based on their contribution in subspace. Therefore, based on the weight value for each band and the threshold, the relevant bands have been adaptively selected. We validated the presented approach on different HSIs and evaluated the obtained results comparing them with different dimensionality reduction techniques.

#### A. TLPP Dimensionality Reduction Approach

In order to keep the initial spatial structure and insure the neighbourhood effects on the one side and use the spectral features on the other side, we propose to use the TLPP as linear projection method [27]. In fact, an HSI is represented with three dimensions, two spatial dimensions (the size of the image) and a spectral one (the number of bands). A third-order tensor can represent the whole HSI denoted by  $R \in \mathfrak{R}^{I_1 \times I_2 \times I_3}$  with elements arranged as  $r_{i_1 i_2 i_3}$ , where  $i_1 = 1, 2, \dots, I_1$ ;  $i_2 = 1, 2, \dots, I_2$ ;  $i_3 = 1, 2, \dots, I_3$  are indexes along each dimension ( $I_1$  and  $I_2$  represent the size of HSI and  $I_3$  represents the number of bands). This tensor representation incorporates the whole HSI with its spatial and spectral features. This tensor representation uses multi-linear algebra and particularly, tensor decomposition and approximation methods. The tensor decomposition is expressed as:

$$R = C \times U^1 \times U^2 \times U^3 \quad (3)$$

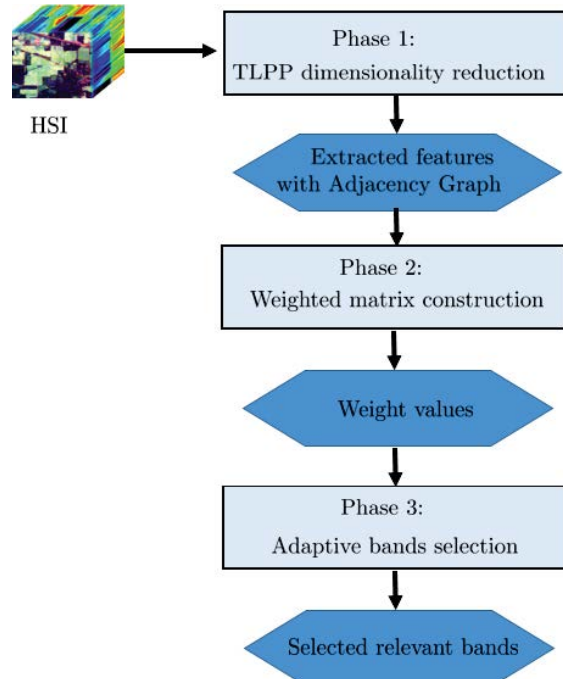


Fig. 1 Flowchart of presented approach

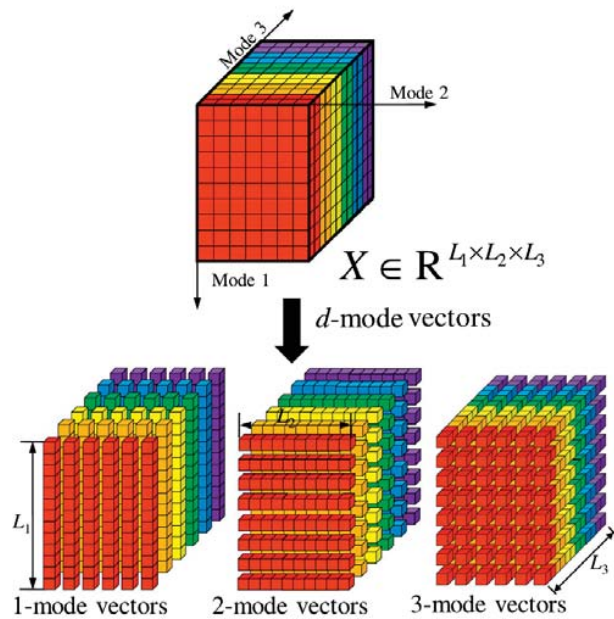


Fig. 2 Illustration of tensor of three modes

where  $C$  is the core tensor, and  $U^n$  is the matrix of eigenvectors associated with the  $n$ -mode covariance matrix  $R_n R_n^T$ . The tensor model can be used in LPP in order to preserve the spatial and spectral information to improve the classification of HSI. The LPP method consists to find the

low-dimensional representation by minimizing the weighted sum of the squared distances between neighbouring data points using a Laplacian graph as:

- 1) Construct an undirected graph  $G = (X, \varepsilon)$  where vertices represent pixels and edges are defined based on proximity between vertices.
- 2) Define weights for the edges in  $\varepsilon$  using one of the following formulas:
  - $W_{i,j} = \exp(-|x_i - x_j|^2 / t)$  if an edge exists between  $x_i$  and  $x_j$  with  $t \in R$  as a heat kernel.
  - $W_{i,j} = 1$  if the vertices  $x_i$  and  $x_j$  are connected, i.e. using a heat kernel  $t = 1$ , and  $W_{i,j} = 0$  otherwise.
- 3) Compute the smallest eigenvalues and eigenvectors of the generalized eigenvector problem:

$$XLX^T a = \lambda DX^T a \quad (4)$$

where  $D$  is the diagonal weighted degree matrix defined by  $D_{i,i} = \sum_j W_{i,j}$  and  $L = D - W$  is the Laplacian matrix which is a positive symmetric matrix. Let the column vector  $a_0, a_1, \dots, a_{m-1}$  be the solution of (4), ordered according to their eigenvalues,  $\lambda_0 < \lambda_1 < \dots < \lambda_{m-1}$ . Thus, the embedding is as:

$$x_i \rightarrow y_i = A^T x_i \quad A = (a_0, a_1, \dots, a_{m-1}) \quad (5)$$

where  $y_i$  is a  $m$ -dimensional vector and  $A$  is a  $n \times m$  matrix. Therefore, when the HSI is reshaped, the formula based on tensor modelling can be defined as:

$$Y_{TLPP} = R \times A^{(3)T} \quad (6)$$

where  $Y_{TLPP}$  is a third-order tensor ( $Y_{TLPP} \in \mathfrak{R}^{I_1 \times I_2 \times d}$ ), holding the  $d$  components and  $A^{(3)T}$  as the eigenvectors.

### B. Weighted Matrix Construction

This phase aims to construct a weighted matrix from the different extracted features based on spectral library obtained from USGS [28]. It consists firstly to compare the different pixels obtained by the adjacency graph in TLPP projection phase with the signatures library using the geodesic distance. We aim to get an affinity matrix from extracted features with  $Y_{TLPP}$ . Hence, we use the above spectral library in order to classify the different pixels and to construct the labeled weighted matrix  $W$ . Thus, it consists to compute the geodesic distance  $\min(d_M(i, j))$  between all pairs of pixels. The nearest pixels from the matrix  $W$  are weighted and labeled using a threshold and the spectral library.

### C. Adaptive Bands Selection

Through the above steps, the HSI can be expressed as  $Y_{TLPP} = TR$  where  $T$  is a projection matrix. In fact, from this equation, it can be observed that  $Y_{TLPP_i}$  is the weighted sum of  $R_1, R_2, \dots, R_d$  with  $d$  is the number of low

dimension and the corresponding weights are  $t_{1i}, t_{2i}, \dots, t_{di}$  which represent the contribution of the corresponding bands to the  $Y_{TLPP}$  components. In other words,  $t_{ji}$  shows how much information the  $j$ th band image contains about the component  $Y_{TLPP_i}$ . Therefore, the importance of each spectral image can be estimated intuitively by calculating the average absolute weight coefficient  $\overline{C}_i$ , which is shown as:

$$\overline{C}_i = \frac{1}{D} \sum_{j=1}^D |t_{ij}| \quad i = 1, 2, \dots, d \quad (7)$$

where  $j$  is the band index and  $d$  the number of components. By sorting the average absolute weight coefficients for all spectral bands, a band weight sequence can be obtained as:

$$[\overline{C}_1 \geq \dots \overline{C}_i \geq \dots \overline{C}_d] \quad (8)$$

In this sequence, the bands with higher average absolute weight coefficients contribute more to the  $Y_{TLPP}$  transformation than other bands do. That means these bands contain more spectral information than other bands. Therefore, the spectral bands with the highest average absolute weight coefficients can be selected and a spectral image with lower dimension is generated with the obtained classified pixels by the spectral library.

## IV. EXPERIMENTS AND DISCUSSION

Here, we validate our presented method with several HSI datasets and present experimental results demonstrating the benefits of TLPP and weighted matrix for HSI semantic interpretation.

### A. HSI Datasets

Two hyperspectral datasets collected by different hyperspectral sensors are used in our experiments.

- 1) The first HSI used in experiments representing the Indiana Pines region in Northwest Indiana was collected by the Airborne Visible/ Infrared Imaging Spectrometer (AVIRIS) sensor in 1992. This HSI contains  $145 \times 145$  pixels with 220 spectral bands covering the range of  $375 - 2500 \text{ nm}$ . The spatial resolution of this HSI is 20 m/pixel. We have used this HSI due to the availability of a reference ground truth image where it consists of 16 ground-truth classes. Fig. 3 shows a color composite image of the Indian Pines data set along with the ground-truth image.
- 2) The second HSI representing the urban area of the Pavia University, Italy was collected by the Reflective Optics System Imaging Spectrometer (ROSIS). Also, this HSI consists of small materials, buildings, and trees. For the spectral resolution, this image contains 115 spectral bands where each band consists of  $610 \times 340$  pixels. The spectral range is from 430 to 860 nm and the spatial resolution is 1.3 m/pixel. This HSI is



collected from an urban area and consequently. Fig. 4 (a) shows a color composite image of University of Pavia, whereas Fig. 4 (b) shows the nine ground-truth classes.

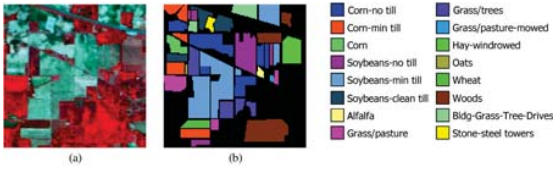


Fig. 3 (a) Color composite image, (b) Ground truth image of Indian Pines

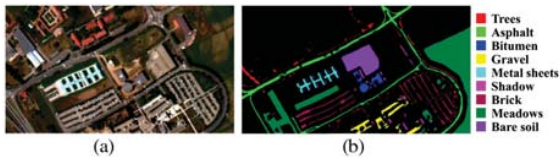


Fig. 4 (a) Color composite image, (b) Ground truth image of University of Pavia

**B. TLPP Dimensionality Reduction**

In our experiment, we used both AVIRIS and ROSIS HSI. Fig. 5 shows the spectral signatures for eight classes extracted from Indian Pines HSI and nine spectral signatures from University of Pavia.

The number of reduced dimensionality has been fixed  $n = 3, 6, 9, 12, 18,$  and  $21$  features. In Indian Pines HSI, better results are given by the presented method with the number of dimensions  $n = 6$ . Also, we have obtained better results of University of Pavia HSI with number of dimensions  $n = 3$ . It appears from the results that the pixels are correctly classified of both HSIs using the spectral library, which is qualified as almost perfect. Fig. 6 compares the scatter plots of the extracted features obtained using TLPP for both HSIs. We can notice out that the presented method TLPP clearly separates the different features.

**C. Adaptive Bands Selection**

After classifying the different pixels from extracted features obtained with TLPP, the presented adaptive bands selection method has been developed to select the relevant bands from the original HSIs according to their contributions coefficients. Tables I and II show the band subset obtained for both HSIs using as well as three other band selection methods, namely CBS, AP and MI with different predefined number of bands ( $n = 3, 6$  and  $15$ ).

After selecting the relevant bands with our presented approach, we have tried to test this performance on classification task. In fact, in Indian Pines HSI, approximately 8600 labeled pixels are employed to train

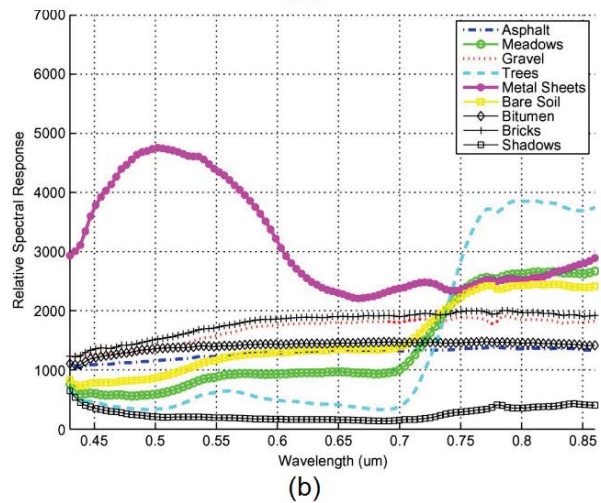
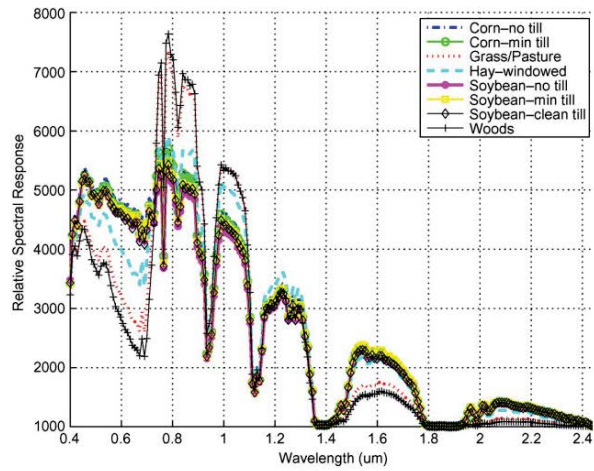


Fig. 5 (a) Spectral signatures of eight classes from Indian Pines (b) Spectral signatures of nine classes from University of Pavia

TABLE I  
SELECTED BANDS USING CBS, AP, MI AND PROPOSED APPROACH FOR INDIANA PINES

number of bands	CBS	AP	MI	Proposed BS
3	29, 167, 174	4, 45, 181	18, 32, 147	9, 16, 189
6	153, 167, 174, 177, 178, 179	4, 9, 16, 177, 178, 181	142, 165, 167, 177, 178, 179	89, 15, 16, 92, 131, 152
15	28, 29, 30, 32, 148, 153, 164, 167, 170, 175, 176, 179, 180, 181, 203	2, 9, 12, 96, 98, 167, 177, 178, 179, 181, 189, 195, 199, 200, 201	17, 29, 30, 36, 143, 154, 156, 162, 169, 170, 181, 189, 195, 197, 201	9, 15, 27, 28, 33, 39, 78, 82, 89, 120, 132, 175, 167, 179, 198

and test the efficacy of the presented system. This dataset is partitioned into approximately 1496 training pixels and 7102 test pixels. Also, the number of training and testing samples used for the University of Pavia dataset are 1476

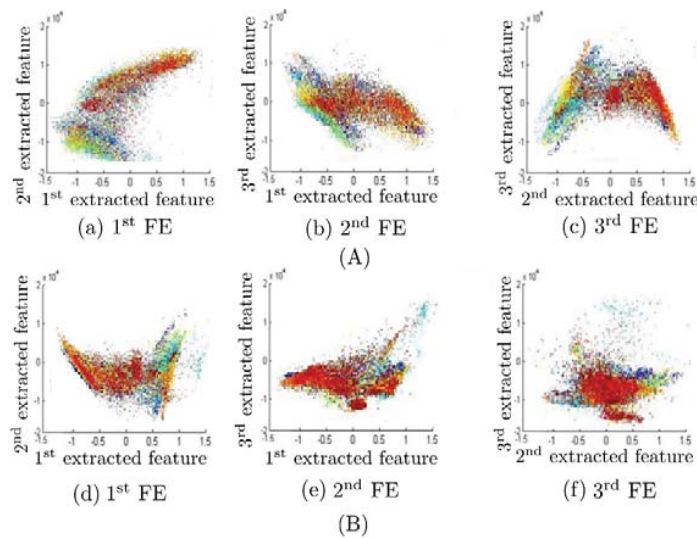


Fig. 6 (A) Obtained extracted features of Indian Pines using TLPP with  $n=3$  (B) Obtained extracted features of University of Pavia using TLPP with  $n=3$

TABLE II  
SELECTED BANDS USING CBS, AP, MI AND PROPOSED APPROACH  
FOR UNIVERSITY OF PAVIA

number of bands	CBS	AP	MI	Proposed BS
3	31, 28, 2	4, 42, 89	72, 101, 14	29, 6, 18
6	101, 28, 24, 17, 78, 79	34, 8, 16, 17, 78, 18	42, 65, 67, 77, 78, 17	29, 6, 18, 22, 13, 154
15	28, 17, 23, 13, 14, 53, 64, 16, 17, 15, 16, 79, 80, 18, 20	42, 29, 81, 29, 19, 67, 77, 78, 19, 18, 89, 95, 59, 20, 21	67, 49, 31, 36, 43, 54, 56, 62, 16, 70, 81, 89, 19, 97, 20	6, 29, 1, 18, 53, 19, 68, 12, 39, 12, 32, 75, 67, 5, 18

and 7380, respectively. We run SVM classifier on the our presented approach and the state of the art methods, i.e., MI, and CBS. Fig. 7 shows the classification accuracy of each band selection method with various numbers of bands.

It is obvious that the presented approach gives better classification rates compared to the other band selection methods. In Indian Pines HSI, the better classification is given by the presented method with the number of dimensions  $n = 6$  and classification accuracy is equal to 95%. Also, we have obtained a better classification of University of Pavia HSI with our presented approach. In fact, the number of dimensions  $n = 3$ , the classification accuracy using our method is approaching to 97%. It appears from the results that the pixels are correctly classified of both HSIs, which is qualified as almost perfect.

#### D. Experimental Time

In this section, the running times (in seconds) spent by each dimensionality reduction technique have been computed. Therefore, the different experiment results are tested and evaluated on a PC with 8-GB memory, 15 CPU and 64-bits Windows 8 OS using MATLAB

2014(b) software. Table III shows the running times for dimensionality reduction. Among these dimensionality reduction methods, PCA is the fastest one. ISOMAP spends the longest time since it needs to compute the nearest neighbors.

TABLE III  
RUNNING TIMES (IN SECONDS) OF DIMENSIONALITY REDUCTION FOR  
THE INDIAN PINES AND THE UNIVERSITY OF PAVIA HSIS USING  
DIFFERENT METHODS

Method	PCA	TLPP	ISOMAP	LPP	CBS	MI	Proposed BS
Indian Pines	0.129	5.022	74.15	22.80	0.325	5.124	4.235
University of Pavia	0.14	12.022	91.95	20.35	0.214	4.951	7.854

#### V. CONCLUSION

In this paper, we have presented an approach for band selection. This approach consists to select the relevant bands from HSI in order to improve the semantic interpretation of HSI. Firstly, the Tensor Locality Preserving Projection (TLPP) and the weight matrix have been used to project the original HSI in subspace and to compute the contribution of each spectral band. Secondly, the different spectral bands have been ranked based on their contribution score and the relevant bands have been adaptively selected for classification task. Finally, the obtained results (bands selection, classification accuracy and the running times) shows the efficiency and the performance of the presented approach compared to many existing dimensionality reduction methods such as PCA, ISOMAP, LPP, etc. As future work, this approach will be extended by adding other knowledge for the semantic interpretation

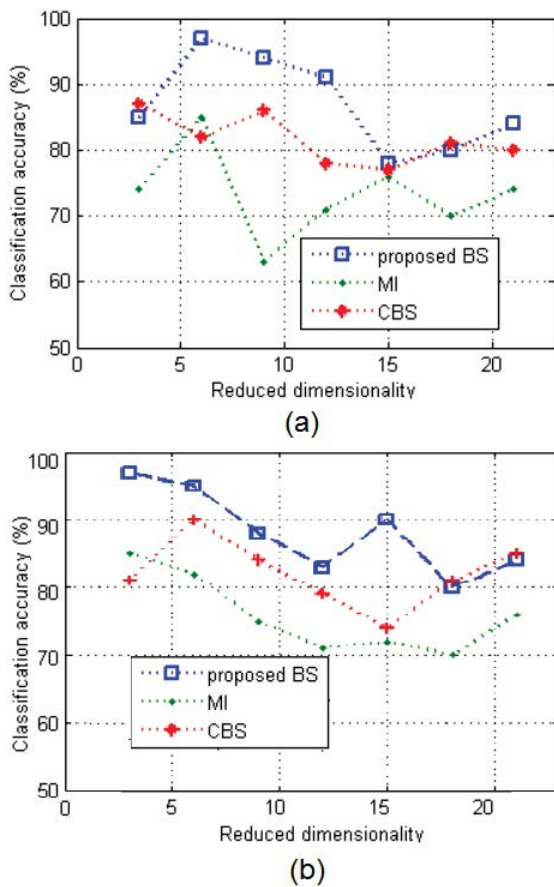


Fig. 7 (a) Classification accuracy of Indiana Pines using different band selection methods (b) Classification accuracy of University of Pavia using different band selection methods

relating to the spatial relations extraction between objects and pixels.

## REFERENCES

- [1] H. Huang, J. Li, and J. Liu, "Enhanced semi-supervised local fisher discriminant analysis for face recognition," *Future Generation Computer Systems*, vol. 28, no. 1, pp. 244–253, 2012.
- [2] S. Chen and D. Zhang, "Semisupervised dimensionality reduction with pairwise constraints for hyperspectral image classification," *Geoscience and Remote Sensing Letters, IEEE*, vol. 8, no. 2, pp. 369–373, 2011.
- [3] H. Huang and M. Yang, "Dimensionality reduction of hyperspectral images with sparse discriminant embedding," *Geoscience and Remote Sensing, IEEE Transactions on*, vol. 53, no. 9, pp. 5160–5169, 2015.
- [4] A. Radoi, R. Tanase, and M. Datcu, "Semantic interpretation of multi-level change detection in multi-temporal satellite images," in *Geoscience and Remote Sensing Symposium (IGARSS), 2015 IEEE International*. IEEE, 2015, pp. 4157–4160.
- [5] M. Ivašić-Kos, M. Pavlič, and M. Matetić, "Data preparation for semantic image interpretation," in *Information Technology Interfaces (ITI), 2010 32nd International Conference on*. IEEE, 2010, pp. 181–186.
- [6] W. Li, S. Prasad, J. E. Fowler, and L. M. Bruce, "Locality-preserving dimensionality reduction and classification for hyperspectral image analysis," *Geoscience and Remote Sensing, IEEE Transactions on*, vol. 50, no. 4, pp. 1185–1198, 2012.
- [7] J. Khoder, R. Younes, and F. B. Ouezdou, "Stability of dimensionality reduction methods applied on artificial hyperspectral images," in *Computer Vision and Graphics*. Springer, 2012, pp. 465–474.
- [8] J. Feng, L. Jiao, F. Liu, T. Sun, and X. Zhang, "Unsupervised feature selection based on maximum information and minimum redundancy for hyperspectral images," *Pattern Recognition*, vol. 51, pp. 295–309, 2016.
- [9] J. M. Sotoca and F. Pla, "Supervised feature selection by clustering using conditional mutual information-based distances," *Pattern Recognition*, vol. 43, no. 6, pp. 2068–2081, 2010.
- [10] B. Guo, R. I. Dampier, S. R. Gunn, and J. D. Nelson, "A fast separability-based feature-selection method for high-dimensional remotely sensed image classification," *Pattern Recognition*, vol. 41, no. 5, pp. 1653–1662, 2008.
- [11] L. Zhang, C. Chen, J. Bu, and X. He, "A unified feature and instance selection framework using optimum experimental design," *Image Processing, IEEE Transactions on*, vol. 21, no. 5, pp. 2379–2388, 2012.
- [12] S. B. Kim and P. Rattakorn, "Unsupervised feature selection using weighted principal components," *Expert systems with applications*, vol. 38, no. 5, pp. 5704–5710, 2011.
- [13] C.-I. Chang and S. Wang, "Constrained band selection for hyperspectral imagery," *Geoscience and Remote Sensing, IEEE Transactions on*, vol. 44, no. 6, pp. 1575–1585, 2006.
- [14] W. Jian, "Unsupervised intrusion feature selection based on genetic algorithm and fcm," in *Information Engineering and Applications*. Springer, 2012, pp. 1005–1012.
- [15] M. Breaban and H. Luchian, "A unifying criterion for unsupervised clustering and feature selection," *Pattern Recognition*, vol. 44, no. 4, pp. 854–865, 2011.
- [16] P. Mitra, C. Murthy, and S. K. Pal, "Unsupervised feature selection using feature similarity," *IEEE transactions on pattern analysis and machine intelligence*, vol. 24, no. 3, pp. 301–312, 2002.
- [17] A. Martínez-UsÓMartinez-Uso, F. Pla, J. M. Sotoca, and P. García-Sevilla, "Clustering-based hyperspectral band selection using information measures," *IEEE Transactions on Geoscience and Remote Sensing*, vol. 45, no. 12, pp. 4158–4171, 2007.
- [18] Y. Qian, F. Yao, and S. Jia, "Band selection for hyperspectral imagery using affinity propagation," *IET Computer Vision*, vol. 3, no. 4, pp. 213–222, 2009.
- [19] B.-C. Kuo, C.-H. Li, and J.-M. Yang, "Kernel nonparametric weighted feature extraction for hyperspectral image classification," *Geoscience and Remote Sensing, IEEE Transactions on*, vol. 47, no. 4, pp. 1139–1155, 2009.
- [20] M. Sugiyama, "Dimensionality reduction of multimodal labeled data by local fisher discriminant analysis," *The Journal of Machine Learning Research*, vol. 8, pp. 1027–1061, 2007.
- [21] P. Deepa and K. Thilagavathi, "Feature extraction of hyperspectral image using principal component analysis and folded-principal component analysis," in *Electronics and Communication Systems (ICECS), 2015 2nd International Conference on*. IEEE, 2015, pp. 656–660.
- [22] L. Ding, P. Tang, and H. Li, "Isomap-based subspace analysis for the classification of hyperspectral data," in *Geoscience and Remote Sensing Symposium (IGARSS), 2013 IEEE International*. IEEE, 2013, pp. 429–432.
- [23] S. Yan, D. Xu, B. Zhang, H.-J. Zhang, Q. Yang, and S. Lin, "Graph embedding and extensions: a general framework for dimensionality reduction," *Pattern Analysis and Machine Intelligence, IEEE Transactions on*, vol. 29, no. 1, pp. 40–51, 2007.
- [24] R. Ji, Y. Gao, R. Hong, Q. Liu, D. Tao, and X. Li, "Spectral-spatial constraint hyperspectral image classification," *Geoscience and Remote Sensing, IEEE Transactions on*, vol. 52, no. 3, pp. 1811–1824, 2014.
- [25] H. Yuan and Y. Y. Tang, "Learning with hypergraph for hyperspectral image feature extraction," *Geoscience and Remote Sensing Letters, IEEE*, vol. 12, no. 8, pp. 1695–1699, 2015.
- [26] N. Renard and S. Bourennane, "Dimensionality reduction based on

tensor modeling for classification methods," *IEEE Transactions on Geoscience and Remote Sensing*, vol. 47, no. 4, pp. 1123–1131, 2009.

- [27] A. Sellami and I. R. Farah, "High-level hyperspectral image classification based on spectro-spatial dimensionality reduction," *Spatial Statistics*, vol. 16, pp. 103–117, 2016.
- [28] R. Clark, "Spectral library," <https://speclab.cr.usgs.gov/spectral-lib.html/>, 2007, (Online; accessed 19-September-2007).



**Akrem Sellami** received the MSc degrees in computer science from the University of Jendouba, Tunisia, in 2012. Currently, he is working toward the PhD degree with the National School of Computer Sciences Engineering, University of Manouba, Manouba, Tunisia. He is also a Permanent Researcher at RIADI Laboratory, University of Manouba, since 2009. His work is mainly related with dimensionality reduction, pattern recognition, signal processing, and machine learning applied to remote sensing

hyperspectral images. He also enjoyed a research scholarship from the ITI Department in Telecom Bretagne where he is currently a Ph.D. student. Mr. Sellami is a member of Arts-Pi Tunisia.



**Imed Riadh Farah** is currently Professor at ISAMM Institute, University of Manouba, Tunisia. He received the Engineer degree in 1991 from ENIG School Engineering, MD degree in 1995 from ISG Institute, and the PhD degree in computer science from National School of Computer Science (ENSI), Tunis, Tunisia in 2003. Since November 2009, he has been Associate Professor and then Professor of computer science. He is an Associate Researcher in the Department ITI-Telecom Bretagne, Brest,

France, since January 2009. Since 2011, he is head of the Higher Institute of Multimedia Art of Manouba (ISAMM). His research interests are artificial intelligence, data mining, image processing, recognition and interpretation, especially for remote sensing applications, and earth observation.



**Basel Solaiman** received the Telecommunication Engineering degree from Ecole Nationale Suprieure des Telecommunications de Bretagne (Telecom Bretagne), Brest, France, in 1983, and the Ph.D. and H.D.R degrees from the University of Rennes I, Rennes, France, in 1989 and 1997. From 1984 to 1985, he was a Research Assistant in the Communication Group at the Centre d'Etudes et de Recherche Scientifique, Damascus, Syria. He joined the Image and Information Processing Department at Telecom Bretagne, in

1992. He is actually the Head of the Image and Information Processing Department at Telecom Bretagne. His current research interests include the fields of remote sensing, medical image processing, pattern recognition, neural networks, and artificial intelligence.